

End Group Effect on the Thermal Response of Narrow-Disperse Poly(*N*-isopropylacrylamide) Prepared by Atom Transfer Radical Polymerization

Yan Xia, Nicholas A. D. Burke, and Harald D. H. Stöver*

Department of Chemistry, McMaster University, Hamilton, Ontario, Canada L8S 4M1

Received September 7, 2005; Revised Manuscript Received December 19, 2005

ABSTRACT: Four series of narrow-disperse poly(*N*-isopropylacrylamide) (PNIPAM) with well-controlled molecular weights and with end groups of varying hydrophobicity were synthesized by room temperature atom transfer radical polymerization in 2-propanol using the corresponding chloropropionate and chloropropionamide initiators. The thermal phase transitions of aqueous solutions of these PNIPAMs were studied by turbidimetry and high-sensitivity differential scanning calorimetry (HS-DSC) and showed an inverse molecular weight (MW) dependence of their cloud points. The magnitude of the MW dependence decreases when using more hydrophobic end groups. The choice of end group further affected the shape of the cloud point curves and the enthalpy of the phase transition. Above the cloud point, narrow-disperse PNIPAM sedimented more rapidly than polydisperse PNIPAM produced by conventional free radical polymerization, especially at concentrations above 1%. Thus, multiple HS-DSC scans of PNIPAM prepared by ATRP typically gave repeatable results only at lower concentrations.

Introduction

Aqueous solutions of poly(*N*-isopropylacrylamide) (PNIPAM) exhibit a reversible thermal phase separation above a critical temperature, known as the lower critical solution temperature (LCST).^{1,2} On the molecular level, this involves a change from solvated random coils below the LCST to tightly packed globular particles above the LCST.^{3–5} This thermoresponsiveness has led to applications in bioengineering^{6–9} and nanotechnology^{10–13} and promises exciting future applications in the area of biosensors and membranes. Much effort has also been invested in better understanding the phase transition behavior and the parameters affecting the phase transition temperature. Most often, this involved studying the cloud point of dilute aqueous PNIPAM solutions, rather than the actual LCST, i.e., the minimum of the two-phase curve in the PNIPAM–water phase diagram.

The molecular weight (MW) dependence of the cloud point of such polymers has been an active yet controversial topic. The cloud points of PNIPAM and related thermoresponsive polymers have been reported to be inversely dependent,^{14–20} directly dependent,^{21,22} or independent^{5,23,24} on the molecular weight. However, most of these studies involved conventionally prepared, polydisperse polymers, which may have precluded precise examination of MW effects. In addition, different initiators, terminators, or chain-transfer agents led to different polymer end groups, which can in turn affect the cloud points.^{22,24–28} Hydrophobic end groups decrease cloud points while hydrophilic end groups tend to increase them, with the magnitude of the effect depending on the nature of the end group. Hydrophobic groups act by increasing the degree of ordering of solvating water while hydrophilic ones tend to decrease the ordering of solvating water. These effects are believed to be greater for hydrophobic/hydrophilic groups located at chain ends rather than midchain.²⁵

End group effects are most pronounced for low MW polymers but have also been reported for polymers with very high MWs.

For example, Saito and co-workers studied several PNIPAM samples prepared with AIBN and one prepared with persulfate initiator.²⁴ They found that the cloud point was constant at 31.5 °C for the AIBN-initiated PNIPAM samples for MW's ranging from 11 to 203 kDa, while the cloud point for the persulfate-initiated sample with MW = 2100 kDa was more than 2 °C higher, which was attributed to the sulfate chain ends in this sample.

In fact, the dependence of cloud point on polymer MW observed in several studies may be attributed, at least in part, to the role of the end group. Polymers with hydrophilic end groups, such as those derived from persulfate initiation or a hydrophilic chain transfer agent, tend to show both higher cloud points and cloud points that drop as the polymer MW increases.^{5,15,17,19}

In contrast, polymers bearing hydrophobic end groups tend to have lower cloud points that are either independent of polymer MW or increase with polymer MW.^{5,21–24} Interestingly, intra- and intermolecular micellization can effectively isolate very hydrophobic groups from water and hence dramatically suppress their hydrophobic effects. For example, alkyl-terminated PNIPAMs can form a hydrophobic core of alkyl chain ends and a diffuse corona of PNIPAM chains when the alkyl end group is long enough to facilitate the micellization.^{25–27,29–31}

Therefore, contributions from the end groups have to be considered when studying the MW dependence of cloud points. Key questions, including the degree to which different hydrophilic and hydrophobic end groups affect the cloud point of polymers with identical MW and how much a single group affects the MW dependence of cloud points, still remain uncertain, largely due to the lack of control over both MW and end group chemistry for PNIPAM. Tanaka and Winnik recently studied the aqueous solution properties of PNIPAMs having two octadecyl end groups, prepared by RAFT polymerization, and observed separate transitions for micellization and chain dehydration.³¹

We recently succeeded in preparing narrow-disperse PNIPAMs by atom transfer radical polymerization (ATRP) and reported

* Corresponding author. E-mail: stoverh@mcmaster.ca.

the MW dependence of their cloud points.³² In contrast to previous studies, the aqueous solutions of these narrow-disperse PNIPAMs showed a dramatic decrease in cloud point with increasing MW. The MW dependence could be seen as a combination of MW and end group effects.

In the present work we take advantage of the simultaneous control over MW and end groups through choice of appropriate ATRP initiators and are now able to resolve the effects of MW and end groups on the cloud points. We first describe the synthesis of narrow-disperse PNIPAMs with different end groups ranging from hydrophilic amide to hydrophobic phenylamide by ATRP using the corresponding initiators. This includes a polymer initiated using *N*-isopropyl-2-chloropropionamide, representing PNIPAM with a hydrogen atom at the initiation end and a chlorine at the termination end. We then report our study of the MW and end group effects on phase transitions of 1% aqueous solutions of these PNIPAMs as determined by turbidimetry and microcalorimetry and show that control of end groups and molecular weight results in sharp thermal transitions that can be tuned from 32 to 70 °C without using comonomers.

Experimental Section

Materials. *N*-Isopropylacrylamide (Aldrich, 97%) was recrystallized twice from benzene/hexane (65:35 v/v) prior to use. Copper(I) chloride (97%), ethyl 2-chloropropionate (97%), 2-chloropropionamide (98%), isopropylamine (99.5+%), aniline (99%), triethylamine (99.5%), 2-chloropropionyl chloride (97%), and tetrabutylammonium bromide (99%) were purchased from Aldrich and used as received. Me₆TREN was prepared as described in the literature.³³ 2-Propanol (*i*-PrOH, Fisher, HPLC grade), *tert*-butyl alcohol (*t*-BuOH, Fisher, Certified), tetrahydrofuran (THF, Caledon, HPLC grade), pentane (Caledon, Reagent grade), methylene chloride (Caledon, Reagent grade), hexanes (Caledon, Reagent grade), and ethyl acetate (Fisher, 99.9%) were used as received. The preparation of polydisperse PNIPAM ($M_{n, GPC} = 28.9$ kDa, $M_w/M_n = 2.0$) by conventional free-radical polymerization using azobisisobutyronitrile (AIBN) was described previously.³²

Synthesis of *N*-Isopropyl-2-chloropropionamide. *N*-Isopropyl-2-chloropropionamide was synthesized by a modification of Brittain's method.³⁴ Isopropylamine (4 mL, 0.05 mol) and triethylamine (14 mL, 0.1 mol) were dissolved in 80 mL of methylene chloride and cooled in an ice bath. After 15 min, 2-chloropropionyl chloride (5 mL, 0.05 mol) dissolved in 20 mL of methylene chloride was added dropwise over 20 min. The reaction was stirred at 0 °C for 30 min and then at room temperature for 3 h. 30 mL of 1 M HCl and three 30 mL aliquots of water were added to dissolve the salt formed during the reaction. The organic layer was washed with two 30 mL aliquots of 5% NaHCO₃ solution and dried over Na₂SO₄. The solvent was removed on a rotary evaporator to yield a deep yellow solid that was recrystallized three times from ethanol/water (7:5 v/v) and passed through a silica column to remove color, using hexane/ethyl acetate (10:1 v/v) as the eluent. The dried sample was recrystallized from ethanol/water and dried under vacuum to afford white crystals (2.9 g, 39% yield). ¹H NMR (CDCl₃): 6.3 ppm (bs, 1H, $-NHCH(CH_3)_2$), 4.35–4.39 ppm (m, 1H, $-CHClCH_3$), 4.03–4.07 ppm (m, 1H, $-CH(CH_3)_2$), 1.72–1.73 ppm (d, 3H, $-CHClCH_3$), 1.18–1.20 (dd, 6H, $-CH(CH_3)_2$); mp: 92.9–93.4 °C (literature mp:³⁵ 96–97 °C).

Synthesis of *N*-Phenyl-2-chloropropionamide. The same procedure used for the synthesis of *N*-isopropyl-2-chloropropionamide was applied to synthesize *N*-phenyl-2-chloropropionamide, yielding a yellow solid. It was purified by recrystallization from ethanol/water (5:2 v/v) to give the product in 42% yield. ¹H NMR (CDCl₃): 8.2 ppm (bs, 1H, $-NHC_6H_5$), 7.15–7.56 ppm (m, 5H, $-NHC_6H_5$), 4.53–4.57 ppm (q, 1H, $-CHClCH_3$), 1.83–1.84 ppm (d, 3H, $-CHClCH_3$); mp: 89.0–89.5 °C (literature mp:³⁶ 82–83 °C).

General Procedure for ATRP of NIPAM. To prepare PNIPAM with a target degree of polymerization of 50, NIPAM (2.00 g, 17.7 mmol), CuCl (0.035 g, 0.35 mmol), and 2-propanol (4.00 g), deoxygenated by bubbling with nitrogen for at least 30 min, were combined and then transferred to a nitrogen-purged 25 mL round-bottom flask fitted with a septum. Me₆TREN (0.081 g, 0.35 mmol) was added via a nitrogen-purged syringe, and the solution was stirred for 20 min to allow formation of the CuCl/Me₆TREN complex. The initiator (0.35 mmol), neat or as a concentrated solution in 2-propanol, was then added using a syringe to begin the polymerization. The reactions were carried out at room temperature under a slight positive pressure of nitrogen.

Aliquots (0.6 mL) were removed at regular intervals and divided between two vials in a 5:1 ratio. The larger portion was accurately weighed, and both portions were dried under a stream of air. The smaller sample was redissolved in THF, passed through a short silica column to remove the catalyst, dried under a stream of air, and used for gel permeation chromatography (GPC) analysis. The larger portion of the aliquot was used to determine conversion: The dried sample was first reprecipitated from THF into pentane (1:12 v/v) and dried to constant weight under vacuum at 60 °C. Conversion was then determined gravimetrically and corrected for residual monomer using ¹H NMR spectroscopy.

Preparation of PNIPAM Oligomer (Targeted Degree of Polymerization ≤ 10). PNIPAM oligomers were prepared following the same procedure as described for ATRP of NIPAM, except that *tert*-butyl alcohol was used as the polymerization solvent. Ethyl 2-chloropropionate was used as the initiator. To reduce the initial radical concentration and thus radical termination, a monomer:solvent ratio of 1:3 was used, and the amount of catalyst and ligand relative to initiator was halved, with monomer:initiator:CuCl:Me₆TREN = 20:2:1:1. Two independent polymerizations were conducted and stopped after 0.5 and 4.6 h, at monomer conversions of 45% and 77%, respectively. Two oligoNIPAM products were thus obtained and designated as oligoNIPAM-4 and oligoNIPAM-10, respectively. As it was difficult to isolate the oligomers by precipitation from the oligomer/monomer reaction mixture, conversion was measured directly by ¹H NMR spectroscopy in D₂O after the sample was air-dried. Here, the peak areas of monomer signals at 5.7 ppm (one proton) or 6.2 ppm (two protons) were compared with the polymer signal at 3.9 ppm (one proton), corrected for contributions due to the monomer.

For isolation, the dried sample dissolved in hexane/THF (5:1 v/v) and passed through a silica column. Monomer eluted first, and the desired oligomer was subsequently eluted using neat THF while the catalyst remained on the silica. The oligomer fractions were dried and redissolved in water and then freeze-dried to yield white powder. These were further dried to constant weight under vacuum at 60 °C.

Polymer Characterization. Average molecular weights and molecular weight distributions were determined on a Waters GPC system consisting of a Waters 515 HPLC pump, a Waters 717plus Autosampler, three Waters Styragel columns (HR2, HR3, and HR4; 30 cm × 7.8 mm; 5 μm particles; exclusion limits: 500–20 000, 500–30 000, and 5000–600 000 g/mol, respectively) maintained at 40 °C, and a Waters 2414 refractive index detector maintained at 35 °C. THF containing 0.25% (w/v) tetrabutylammonium bromide was used as the mobile phase (0.8 mL/min), and the system was calibrated with narrow-disperse polystyrene standards.

¹H NMR spectra were measured on Bruker AV 200 or DRX 500 spectrometers with samples dissolved in D₂O.

Determination of Phase Transitions in Aqueous Solutions. Cloud points were measured on a Cary 100 Bio UV–vis spectrophotometer equipped with a temperature-controlled, six-position sample holder. Aqueous PNIPAM solutions (1 wt %) were heated at 0.2 °C/min while both the transmittance at 500 nm (1 cm path length) and the solution temperature, as determined by the internal temperature probe, were monitored.

HS-DSC was performed on a MicroCal VP-DSC microcalorimeter to measure the phase transition temperature of 1 wt % PNIPAM solutions. Samples were degassed and transferred to the 0.5121 mL

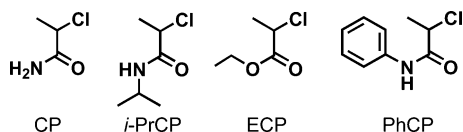


Figure 1. Chemical structures of 2-chloropropionamide (CP), isopropyl 2-chloropropionamide (*i*-PrCP), ethyl 2-chloropropionate (ECP), and phenyl 2-chloropropionamide (PhCP).

sample cell (tantalum wall) by syringe. Samples were scanned at a constant heating rate which was varied from 15 to 60 °C/h at an external pressure of 170 kPa. After each run, the sample cell was cleaned by flushing with 300 mL of distilled water, then with 10 mL of methanol, and finally with 600 mL of distilled water to remove residual methanol. The DSC was calibrated by supplying a precisely known current to the reference cell of the microcalorimeter.

Results and Discussion

ATRP of NIPAM with Different Initiators. PNIPAMs with different end groups were synthesized by ATRP employing a series of initiators so as to produce end groups varying in hydrophobicity. ATRP of acrylamides has suffered from lack of control and from low conversions, mainly attributed to the competitive coordination of their amide groups with the metal catalysts.^{34,37–39} In our previous polymerizations of *N,N*-dimethylacrylamide (DMA)⁴⁰ and NIPAM³² by ATRP, we used alcohols as polymerization solvents on the hypothesis that they might protect the catalyst by hydrogen bonding to the amide groups of both monomer and polymer. ATRP of NIPAM in 2-propanol was found to give good control and high conversions,³² and this solvent was hence used again in this work. 2-Chloropropionates or 2-chloropropionamides were used together with CuCl as catalyst and Me₆TREN as ligand at 1:1:1 ratios to initiate polymerizations, based on previous studies.^{32,34,37–40} Specifically, 2-chloropropionamide (CP), *N*-isopropyl-2-chloropropionamide (*i*-PrCP), ethyl 2-chloropropionate (ECP), and *N*-phenyl-2-chloropropionamide (PhCP) were chosen as initiators to give polymers with end groups of varying polarity, ranging from hydrophilic for CP to hydrophobic for PhCP (Figure 1).

Monomer conversion and polymer molecular weight were determined at different stages during each polymerization. Conversions were determined gravimetrically. Polymer molecular weights (MWs) and polydispersity indices (PDIs) were determined by a GPC method developed by Müller.⁴¹ This method had been established to give reproducible results, though with MW values significantly higher than those obtained from

MALDI–TOF analysis,⁴¹ and therefore, the MW values determined by GPC in our work were only used to reveal trends. ¹H NMR spectroscopy was also used to obtain molecular weights of ECP and PhCP initiated polymers by comparing the peak areas of the polymer isopropyl C–H signal at 3.9 ppm, with the ethoxy signal at 4.1 ppm (O–CH₂–) and the aromatic signal at 7.2–7.4 ppm arising from ECP and PhCP, respectively. The MWs of CP and *i*-PrCP initiated polymers could not be determined by NMR due to the overlap of end group signals with those of the main chain. The M_n values determined by either GPC ($M_{n,GPC}$) or NMR ($M_{n,NMR}$) increased in proportion to the monomer:initiator (M:I) ratio (Table 1), and $M_{n,NMR}$ values were in good agreement with theoretical values.

As summarized in Table 1, polymerizations with all of the initiators gave moderate to high conversions for target degrees of polymerization (DPs) of 50, 100, and 200. Data for methyl 2-chloropropionate (MCP)-initiated polymerizations described in our previous report³² have been included for comparison. When DP = 200 was targeted, monomer concentration was increased to 50% to speed up polymerization and promote monomer conversion. Polymerizations with target DP of 50 were used to study the kinetics of the ATRP. We observed almost no differences in the kinetic characteristics of these four polymerizations, showing that changing the substitution pattern on the propionyl fragment of the initiators did not affect the initiation or the propagation (Figure 2). Similar to our previous work on the ATRP of NIPAM using MCP initiator, first-order kinetic plots showed slight curvature especially in the early stage of polymerization, which had been attributed to progressive catalyst deactivation rather than chain termination. The linear molecular weight ($M_{n,GPC}$) increase with conversion and the low PDIs (1.0–1.2) throughout the polymerization revealed good control in all the polymerizations.

Therefore, 2-propanol has proven to be an effective solvent for the ATRP of NIPAM, suitable for a range of initiators, giving good conversion, controlled MW, and low PDI. The apparent M_n values measured by GPC were about 2–3 times higher than expected, as also reported by Müller's group.⁴¹ The MWs of these new PNIPAMs as measured by GPC are somewhat higher than those reported previously for the MCP initiator.³² This is attributed to a deterioration of the GPC columns in the intervening time, as a sample originally prepared using MCP now also showed an analogously higher MW.

Thermal Phase Transitions by Turbidimetry. Four PNIPAM samples of each end group type were prepared to study their thermal phase transitions as a function of $M_{n,th}$ ranging from

Table 1. Monomer Conversion, Molar Mass (M_n), and Polydispersity (M_w/M_n) Data for Atom Transfer Radical Polymerization (ATRP) of *N*-Isopropylacrylamide (NIPAM) in 2-Propanol with Different Initiators^a

initiator	[M] ₀ : [I] ₀ (M/solvent) (w/w)	time (h)	conv (%)	$M_{n,th}^b$	$M_{n,GPC}^c$	$M_{n,NMR}^d$	M_w/M_n^c
CP	50:1 (1/2)	4.5	80	4500	11400		1.07
	100:1 (1/2)	7.6	78	8800	19100		1.08
	200:1 (1/1)	5.1	72	16300	57000		1.09
<i>i</i> -PrCP	50:1 (1/2)	4.5	87	4900	11100		1.11
	100:1 (1/2)	7.2	78	8800	20500		1.14
	200:1 (1/1)	5	85	19200	58400		1.12
ECP	50:1 (1/2)	4.5	81	4600	9700	4300	1.06
	100:1 (1/2)	7	79	8900	21000	7300	1.10
	200:1 (1/1)	5	79	17900	45100	15200	1.13
PhCP	50:1 (1/2)	4.5	82	4600	12500	4800	1.08
	100:1 (1/2)	7.6	85	9600	25000	9300	1.11
	200:1 (1/1)	5.1	81	18300	49900	18100	1.12
MCP ^e	50:1 (1/2)	4	89	5000	8000	5000	1.15
	100:1 (1/2)	7	91	10300	17300	8400	1.13
	200:1 (1/1)	4.5	78	17600	44200	16400	1.14

^a Experimental conditions: typically 2 g of NIPAM; initiator:CuCl:Me₆TREN = 1:1:1; room temperature. ^b $M_{n,th} = M_{NIPAM}[NIPAM]_0 \text{conv}/[\text{initiator}]_0$. ^c From GPC in 0.25% (w/v) Bu₄NBr/THF. ^d From ¹H NMR spectroscopy (500 MHz) in D₂O, 25 °C. ^e Data from ref 32.

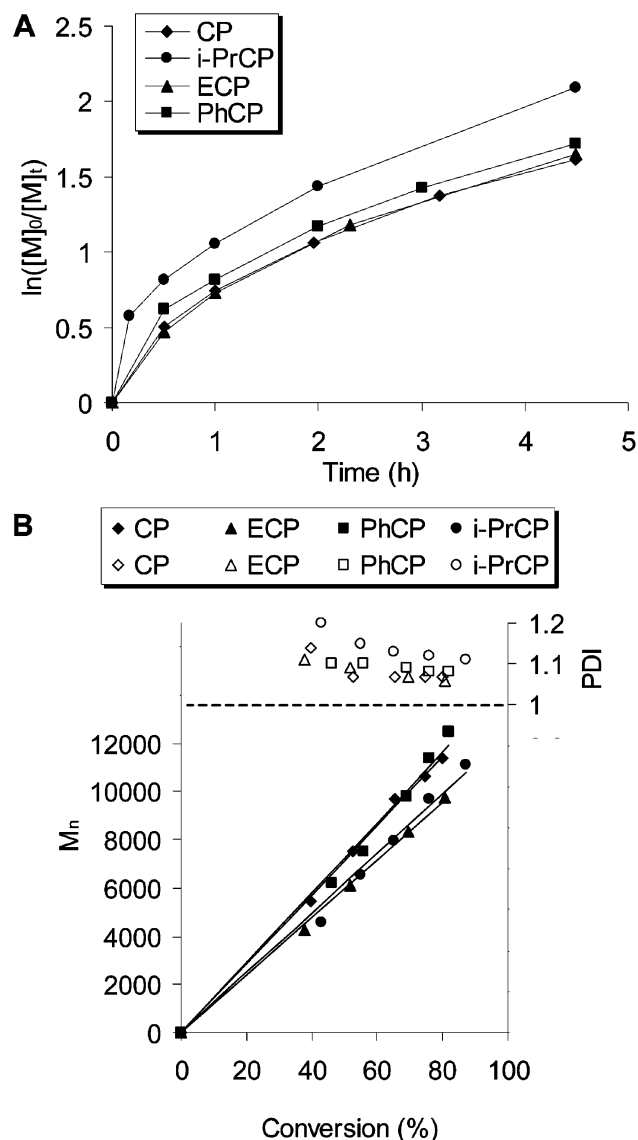


Figure 2. (A) Kinetic plot for the ATRP of NIPAM in *i*-PrOH with different initiators. (B) Dependence of molecular weight ($M_{n, GPC}$) and polydispersity (M_w/M_n) on conversion. Conditions: NIPAM/*i*-PrOH = 1/2 (w/w); NIPAM:initiator:CuCl:Me₆TREN = 50:1:1:1; room temperature. The lines in (A) serve as guides for the eye while those in (B) are best-fit lines.

~3 to ~20 kDa. Each sample was designed to have MW similar to those of their counterparts in other end group types, so that the end group effect could be studied independent of the MW.

Cloud points of 1 wt % aqueous solutions of these PNIPAMs were measured by turbidimetry. Transmittance of the solution was recorded with increasing temperature. A slow heating rate of 0.2 °C/min was used in all the measurements to minimize the thermal lag between the sample cell and the solution. The cloud point of each sample was determined as the average of at least two independent scans. Typically, the cloud points of independent scans varied by less than 0.3 °C.

Table 2 summarizes turbidimetry results, and Figure 3 shows the transmittance vs temperature plots (cloud point curves) for all the PNIPAMs with four different end groups. The polymers are designated by attaching the initiator used, namely, as PNIPAM-CP, PNIPAM-*i*-PrCP, PNIPAM-ECP, and PNIPAM-PhCP. PNIPAM-CP and PNIPAM-*i*-PrCP polymers showed sharp transitions, while PNIPAM-ECP and -PhCP showed apparent early onsets in their cloud point curves similar to that

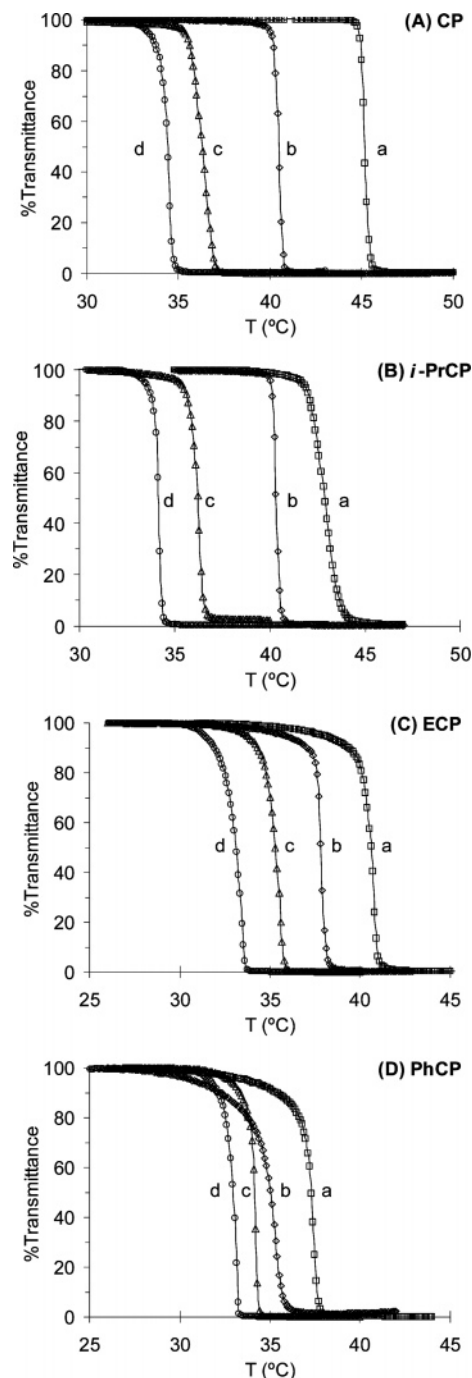


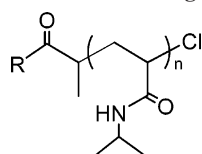
Figure 3. Transmittance vs temperature for 1 wt % solutions of PNIPAM made by ATRP with the initiator (A) CP: $M_{n, th}$ = (a) 3.0, (b) 4.5, (c) 8.8, (d) 16.3 kDa; (B) *i*-PrCP: $M_{n, th}$ = (a) 3.1, (b) 4.9, (c) 8.8, (d) 19.2 kDa; (C) ECP: $M_{n, th}$ = (a) 2.9, (b) 4.6, (c) 8.9, (d) 17.9 kDa; (D) PhCP: $M_{n, th}$ = (a) 3.2, (b) 4.6, (c) 9.6, (d) 18.3 kDa. Heating rate = 0.2 °C/min.

previously observed for PNIPAM-MCP.³² These early onsets are most significant for low-MW PNIPAMs and can start as much as 5 °C below the main transition, as seen for the PNIPAM-PhCP, which bears the most hydrophobic end group. However, the oligomers of PNIPAM-ECP discussed below do not show any such early onset, indicating that these early onsets, as well as the widths of the cloud point curves, are likely not due to either the hydrophobic end groups or micellization of low molecular weight fractions, but rather to differences in the rates of aggregation of the different PNIPAMs, which is beyond the scope of this study. To avoid interference from these effects,

Table 2. Properties of Various PNIPAMs with Different Molar Mass (M_n) and End Groups in Aqueous Solution^a

R	$M_{n,th}$ (Da)	$M_{n,GPC}$ (Da)	$M_{n,NMR}$ (Da)	PDI	phase transition temp (°C)		ΔH^c (kcal mol ⁻¹)
					turbidity ^b (90/50% T)	HS-DSC ^c ($T_m/T_{1/2}$)	
-NH ₂	3000	7500		1.07	44.9/45.3	48.4/6.8	1.04
	4500	11400		1.07	40.2/40.7	42.9/4.6	1.34
	8800	19100		1.08	35.6/36.3	39.0/2.8	1.39
	16300	57000		1.09	33.8/34.4	36.1/2.1	1.58
-NH- <i>i</i> -Pr	3100	6500		1.15	42.0/42.9	47.1/7.8	1.01
	4900	11100		1.11	40.1/40.3	42.2/4.3	1.24
	8800	20500		1.14	34.7/36.0	38.1/2.6	1.39
	19200	58400		1.12	33.7/34.1	35.4/2.0	1.61
-OEt	2900	6100	3000	1.09	39.3/40.6	42.2/6.2	1.33
	4600	9700	4300	1.06	37.1/37.8	39.7/3.4	1.33
	8900	21000	7300	1.10	33.9/35.2	37.0/2.6	1.46
	17900	45100	15200	1.13	31.9/33.3	35.0/1.9	1.62
-NHPh	3200	7500	3200	1.10	35.4/37.4	39.2/4.2	1.32
	4600	12500	4800	1.08	32.2/35.1	37.6/3.3	1.33
	9600	25000	9300	1.11	33.3/34.2	35.6/2.4	1.49
	18300	49900	18100	1.12	32.0/32.8	34.2/1.9	1.55
-OMe ^d	3300	4600	2800	1.07	36.3/43.0		
	5000	8000	5000	1.15	37.5/38.9		
	8600	14300	6700	1.13	36.1/36.4		
	17600	35600	15700	1.13	34.4/34.6		

^a Parameters defined in Table 1. ^b 1 wt % solution; heating rate = 0.2 °C/min. ^c 1 wt % solution; heating rate = 1.0 °C/min; values are kilocalories per mole of monomer repeating units. ^d Data from ref 32.

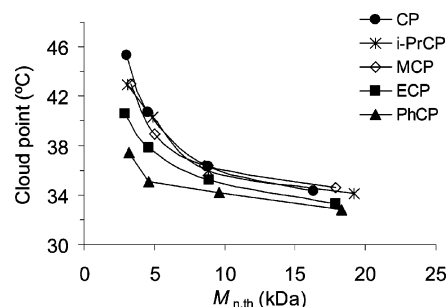
Scheme 1. Structure of PNIPAM with Controlled End Groups and Molecular Weight

we use the 50% transmittance points (50% T) to determine the cloud point and additionally provide the 90% T point to give an indication of the width of the transition.

For each end group, the polymers showed inverse MW dependence of the cloud point (Figure 4). For instance, the cloud point (50% T) of PNIPAM-CP polymers dropped from 45.3 to 34.4 °C as the MW ($M_{n,th}$) increased from 3.0 to 16.3 kDa, while for PNIPAM-PhCP, the cloud point dropped from 37.4 to 32.8 °C as the MW ($M_{n,th}$) increased from 3.2 to 18.3 kDa.

The end group effect was most significant for the low-MW samples. PNIPAM-*i*-PrCP, designed to have no initiator end group effect and hence represent an ideal PNIPAM, had a cloud point of 42.9 °C at 3 kDa MW. In comparison, the hydrophilic propionamide end group elevated the cloud point to 45.3 °C, while the hydrophobic ethoxypropionate and phenylpropionamide end groups lowered the cloud point to 40.6 and 37.4 °C, respectively. Thus, a 7.9 °C drop in cloud point was caused by the addition of a phenyl group at the chain end. Similarly, changing the ester substituent from methyl (PNIPAM-MCP) to ethyl (PNIPAM-ECP) lowered the cloud point by 2.4 °C for the 3 kDa chains. PNIPAM-MCP had cloud points similar to those of PNIPAM-*i*-PrCP, indicating that the weakly hydrophobic methyl propionate end group does not have a significant effect on the cloud point, at least in the MW range studied.

The end group effect is much less remarkable for longer chains. For samples having MW around 16–18 kDa, the cloud point only decreased 1.6 °C from 34.4 °C for PNIPAM-CP to 32.8 °C for PNIPAM-PhCP. Clearly, the MW dependence of the cloud point is a combination of the end group effect and the MW effect. Hydrophilic end groups exacerbate the MW effect, while hydrophobic end groups can mitigate the MW dependence or perhaps reverse it if the end group were hydrophobic enough. PNIPAM-PhCP gave the smallest MW dependence among the four series studied here. However, in

**Figure 4.** Cloud point (50% T) vs polymer molecular weight ($M_{n,th}$) for narrow-disperse PNIPAM samples with different end groups made by ATRP. Cloud points determined by turbidimetry on 1 wt % solutions. Heating rate = 0.2 °C/min.

the range of MWs and end groups studied, the MW effect still dominates, such that all the chains show an inverse MW dependence. PNIPAM-*i*-PrCP polymers are considered to have no end group effect except the chlorine at the terminating end, so these polymers most closely reflect the authentic MW effect.

NIPAM Oligomers. Two oligoNIPAM samples with degrees of oligomerization of 10 (oligoNIPAM-10, $M_{n,GPC}$ = 2530, $M_{n,NMR}$ = 1070, PDI = 1.20) and 4 (oligoNIPAM-4, $M_{n,NMR}$ = 460) were prepared with the ECP initiator in order to extend the cloud point study to very low molecular weights. The GPC traces are shown in Figure 5A. The bimodal MW distribution of oligoNIPAM-4 might be due to the improved GPC resolution at the low MW end, which enables resolution of individual oligomers with different DP, or due to rapid termination from high radical concentration at the initiation.

Turbidimetry showed that oligoNIPAM-10 has a cloud point of 50.9 °C and oligoNIPAM-4 has a cloud point of 70.4 °C. OligoNIPAM-10 still has a sharp transition, but oligoNIPAM-4 has a very broad transition in transmittance over 10 °C (Figure 5B). In both cases, the transmittance decreased to about 10% before increasing again, which indicates aggregation and/or settling of the sample, resulting in less light being scattered. This is commonly seen for all the samples, but it is more rapid for these oligomers.

High-Sensitivity Differential Scanning Calorimetry (Microcalorimetry). High-sensitivity differential scanning calorimetry (HS-DSC) was also used to investigate the phase

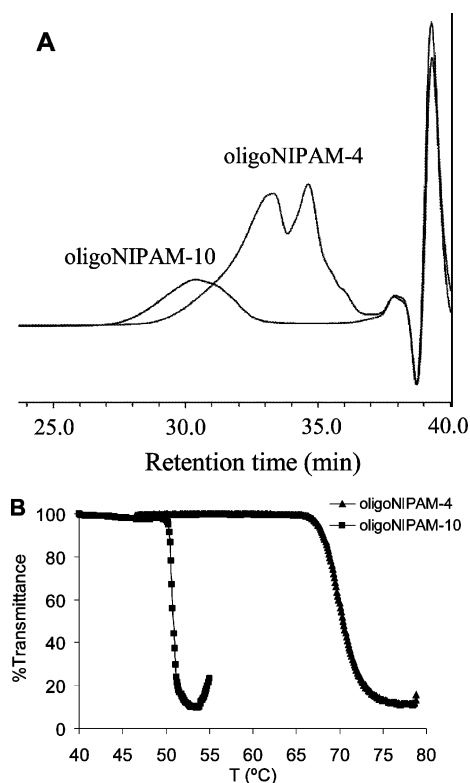


Figure 5. NIPAM oligomers initiated with ECP: (A) GPC traces; (B) cloud point curves (transmittance vs temperature) for 1 wt % solutions.

transition of these polymer solutions. HS-DSC records the changes of partial excess heat capacity C_p of the solutions as a function of temperature. It has been widely used to study the “coil-to-globule” transition of PNIPAM^{5,14,28,42,45} and other thermoresponsive polymers^{5,16,18,20,28,43} and their hydrogels⁴⁴ and to provide information about the peak temperature and the enthalpy change of the phase transition. It has been widely claimed that varying the scanning rate over a wide range has little or no effect on the shape of the thermograms or the transition temperature.^{5,14,20,28,42–44} For example, Winnik et al.^{20,31,43} (10–90 °C/h) and Mikheeva et al.⁴⁴ (15–120 °C/h) found no effect of heating rate, while Zhu et al.¹⁶ observed only a slight upward shift of the transition temperature when the scanning rate was increased 10-fold. Conversely, Ding et al. recently reported that the phase transition temperature increased linearly with the heating rate, rising by 1.0 °C as the heating rate went from about 5 to 90 °C/h.⁴⁵ This was attributed to more intrachain contraction and less interchain association in a fast heating scan.⁴⁵ The reproducibility of the results was demonstrated in these previous studies by repeated scans at the same heating rate. Therefore, it is commonly concluded that the heat transfer in microcalorimetry is so effective that the characteristic times of the transitions of polymers are shorter than those of the thermal equilibration of the cells.

To verify that the calorimetric measurements were independent of the heating rate and therefore were thermodynamic parameters, the heating rate dependence and reproducibility of the thermograms were studied. 1 wt % aqueous PNIPAM solutions were held in a 0.5121 mL DSC cell and scanned sequentially with heating rates of 15, 30, and 60 °C/h. Before each heating scan, the sample was held at 10 °C for 10 min. All samples were cooled at 90 °C/h unless indicated, and only heating scans were considered.

We observed that changing the heating rate from 15 to 60 °C/h did not affect the peak temperature, T_m , but only slightly broadened the peak for a polydisperse PNIPAM ($M_{n,GPC} = 28.9$ kDa, $M_w/M_n = 2.0$) made by AIBN-initiated polymerization. However, for PNIPAM made by ATRP, slow heating rates or holding the sample above the LCST resulted in the formation of an extra peak at the low-temperature side of the original transition in subsequent scans. Low-MW samples were found more vulnerable to this change than high-MW ones. It hence appears that PNIPAMs made by ATRP are not colloiddally stable and may sediment. The concentrated phase resulting from sedimentation may cause the extra peaks seen in subsequent DSC runs of the same sample. It also appears that the sedimented polymer is slow to redisperse. Extensive incubation (10 h) in the DSC cell at 10 °C reduces but does not completely remove the extra peak. The apparent rapid sedimentation and slow redispersal of the narrow-disperse PNIPAM samples are in marked contrast to the behavior observed in most studies. This behavior may be due to the low molecular weight and the narrow MW distribution of the PNIPAM samples made by ATRP.

Particular care is thus required to perform microcalorimetry on such PNIPAM solutions. To avoid the appearance of the secondary, low-temperature peak, we only used the result from the first heating scan of every sample and a heating rate of 60 °C/h for our measurements. The endotherm maximum, onset, and width were not significantly altered when slower scan rates (15, 30 °C/h) were used. The reproducibility of the results was within 0.5 °C, checked by repeating measurements with freshly prepared sample solutions. The DSC results are summarized in Table 2, and the microcalorimetric endotherms for each family of PNIPAMs are shown in Figure 6.

Microcalorimetry results showed the same tendency of MW effect and end group effect as revealed by turbidimetry. Hydrophobic end groups decreased the transition temperature while the hydrophilic amide end group increased the transition temperature. All PNIPAMs in our study had inverse MW dependence. The peak temperature, T_m , from microcalorimetry of each sample was 2–3 °C higher than its cloud point measured by turbidimetry. DSC peaks broadened from about 2 °C in the peak width at half-height, $T_{1/2}$, for the longest chain to 4–7 °C for the shortest, despite similar PDI values. This is not surprising as in the low MW range the phase transition temperature is more sensitive to MW changes, so residual polydispersities play a more important role.

While in the cloud point curves measured by turbidimetry, PNIPAM-CP and PNIPAM-*i*-PrCP had sharper transitions than the PNIPAMs with hydrophobic end groups, the DSC studies showed PNIPAM-CPs to have the broadest phase transitions. The polar CP end group increases the phase transition temperature, especially for the low-MW fractions. In cloud point measurements, this effect can be masked by the dominant high-MW fractions that phase separate first. In HS-DSC, the phase separation of these low-MW fractions is detected and results in a broader distribution after T_m in the thermogram. Hence, a sharper transition in the cloud point curve does not necessarily indicate a narrower real thermal phase transition.

The enthalpy of phase transition (ΔH) exhibited a slight direct MW dependence regardless of end group down to $M_{n,th} \sim 5$ kDa. ΔH decreased from 1.6 kcal mol^{−1} for the longest chains ($M_{n,th} \sim 18$ kDa) to 1.3 kcal mol^{−1} for the second shortest chains ($M_{n,th} \sim 5$ kDa). Interestingly, when the MW further decreased from 5 to 3 kDa, for PNIPAM with hydrophobic end groups, PNIPAM-ECP and PNIPAM-PhCP, ΔH remained constant at

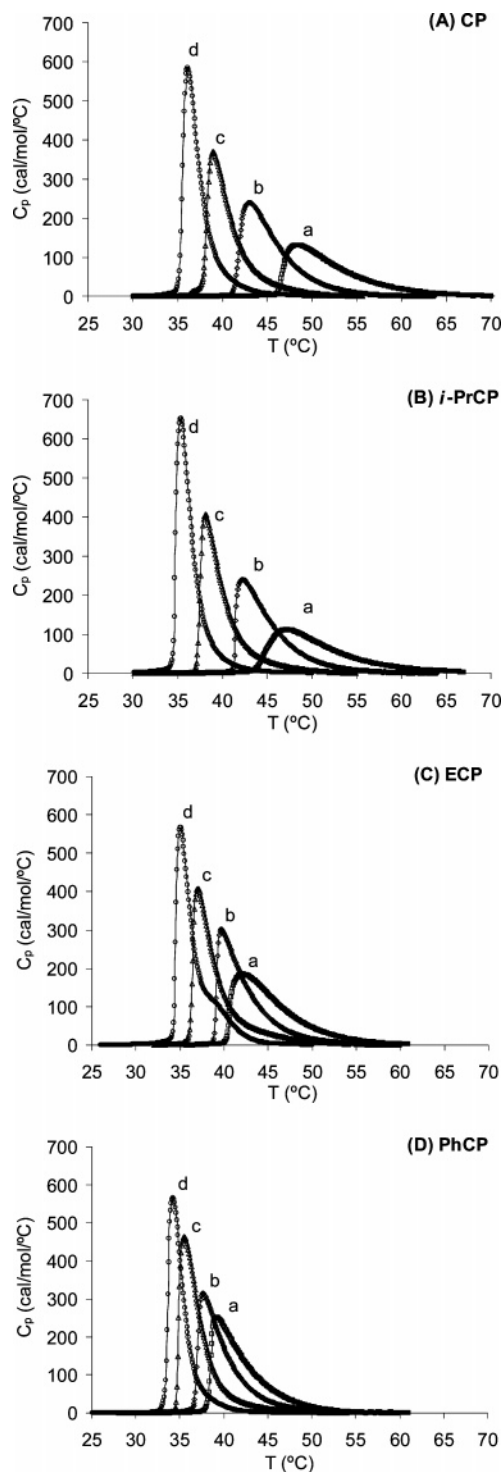


Figure 6. Microcalorimetric endotherms of 1 wt % aqueous solutions of (A) PNIPAM-CP, $M_{n,th}$ = (a) 3.0, (b) 4.5, (c) 8.8, (d) 16.3 kDa; (B) PNIPAM-*i*-PrCP, $M_{n,th}$ = (a) 3.1, (b) 4.9, (c) 8.8, (d) 19.2 kDa; (C) PNIPAM-ECP, $M_{n,th}$ = (a) 2.9, (b) 4.6, (c) 8.9, (d) 17.9 kDa; (D) PNIPAM-PhCP, $M_{n,th}$ = (a) 3.2, (b) 4.6, (c) 9.6, (d) 18.3 kDa. Heating rate = 60 °C/h.

$\sim 1.3 \text{ kcal mol}^{-1}$. In contrast, PNIPAM with hydrophilic end groups, PNIPAM-*i*-PrCP and PNIPAM-CP, showed a sudden decrease in ΔH from 1.3 to 1.0 kcal mol^{-1} (Figure 7). This difference may reflect the end group effect on the thermal phase transition. Hydrophobic end groups may help the desolvation of the polymers above the cloud point, while hydrophilic end groups may interfere with it. For example, the low-MW fraction of PNIPAM-CP ($M_n \sim 3 \text{ kDa}$) may not undergo phase transition

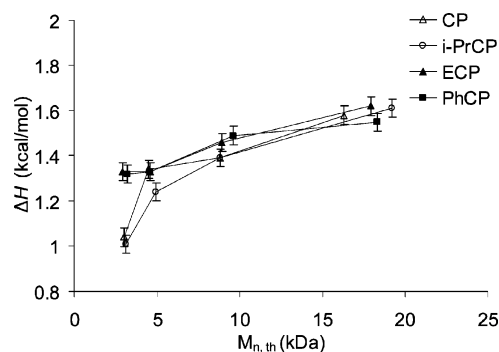


Figure 7. Plots of the enthalpy of transition as a function of molecular weight of 1 wt % aqueous solution of the PNIPAM made by ATRP with different initiators. Heating rate = 60 °C/h.

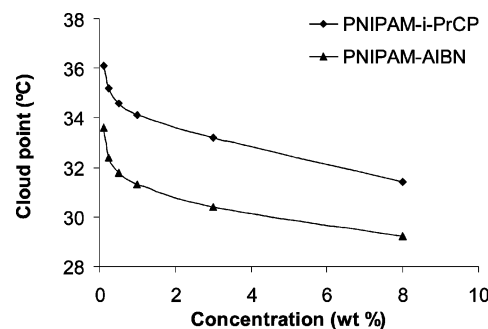


Figure 8. Effect of polymer concentration on the phase separation temperature of aqueous solutions of PNIPAM-*i*-PrCP ($M_{n,th} = 19.2 \text{ kDa}$) and PNIPAM-AIBN ($M_{n,GPC} = 28.9 \text{ kDa}$) as measured by turbidimetry.

during heating leading to a 20% lower apparent ΔH . This effect may only manifest in very low-MW samples, where the end groups are present in significant proportion relative to the monomer units along the chain.

The ΔH values obtained in this work are within the range 0.8–1.9 kcal mol^{-1} reported for linear PNIPAM.^{5,14,20,24,30,42,43,45} Winnik et al. reported a strong direct dependence of ΔH on MW for narrow-disperse thermoresponsive poly(2-isopropyl-2-oxazoline),⁴³ and Zhu et al. reported a significant inverse dependence of ΔH on MW over a much wider MW range for thermoresponsive poly(*N,N*-diethylacrylamide),¹⁶ while other reports do not seem to present a clear MW dependence.^{5,14,20,24}

Effect of Polymer Concentration. The concentration dependence of the phase transition was studied using two samples: one prepared by ATRP (PNIPAM-*i*-PrCP, $M_{n,th} = 19.2 \text{ kDa}$) and the other prepared using AIBN ($M_{n,GPC} = 28.9 \text{ kDa}$, $M_w/M_n = 2.0$). They both showed the same trend over the concentration range of 0.1–8%: as the concentration increases, their cloud points decrease (Figure 8), demonstrated by turbidimetry for both (Figure 9) and HS-DSC for PNIPAM-*i*-PrCP (Figure 10). The concentration dependence is stronger in the dilute range below 1 wt %. The cloud point curves showed that more concentrated samples tend to aggregate and settle more easily, resulting in an increase in transmittance shortly after the initial decrease. In addition, the samples made by ATRP tend to settle more readily than the one made using AIBN (Figure 9). This supports our hypothesis that the change in the DSC thermogram of samples made by ATRP may be caused by the more efficient aggregation and settling of PNIPAM above the LCST.

PNIPAM made with persulfate initiator has been found to form stable colloidal suspensions upon heating^{46,47} where the charged sulfate end group provides colloidal stability. PNIPAM and another thermoresponsive polymer, poly(*N*-vinylcaprolac-

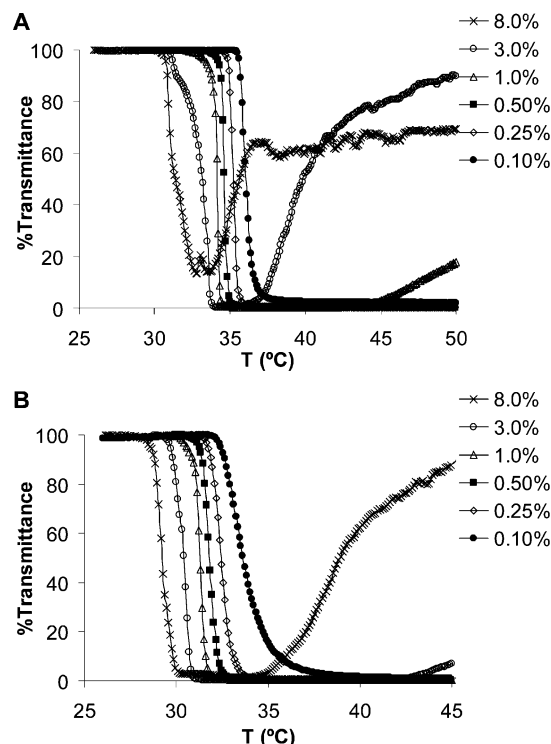


Figure 9. Transmittance vs temperature for aqueous solutions of (A) PNIPAM-*i*-PrCP ($M_{n,th} = 19.2$ kDa) and (B) PNIPAM-AIBN ($M_{n,GPC} = 28.9$ kDa) with different concentrations.

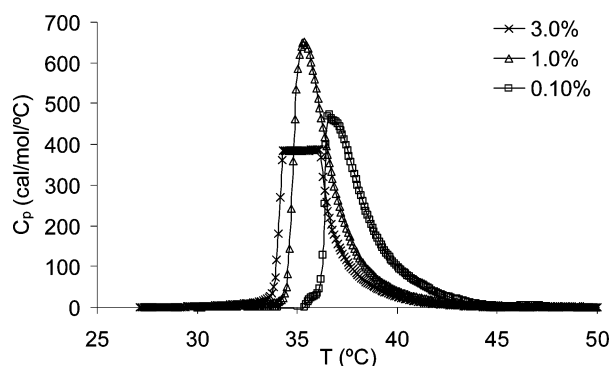


Figure 10. Microcalorimetric endotherms of aqueous solutions of PNIPAM-*i*-PrCP ($M_{n,th} = 19.2$ kDa) with different concentrations. (Note: the 3.0% PNIPAM sample exceeded the upper detection limit of the HS-DSC and went off scale.)

tam) (PVCL), prepared with neutral initiator AIBN were also observed by light scattering (LS) to give aggregates with constant hydrodynamic radius when held above their LCST for days.^{20,48} It was also found that low-MW samples lead to larger aggregate size, and this was interpreted as due to partially solvated chains on surfaces of the aggregates providing steric stabilization against further aggregation. The polymer concentrations in these LS studies are at least 10-fold lower than in our experiments, making flocculation less favorable. Our low-MW, narrow-disperse PNIPAM samples were observed to sediment faster and hence be less colloidal stable than the polydisperse PNIPAM-AIBN. The role of MW and polydispersity upon the aggregation and colloidal stability of PNIPAM solutions will be the subject of future studies.

Conclusion

We have successfully prepared several series of narrow-disperse PNIPAM with end groups of varying polarity by ATRP, using the corresponding chloropropionate and chloropropiona-

mide initiators. Improved control over MW and end groups enabled the resolution of MW and end group effects on the thermal transitions of their aqueous solutions as measured by turbidimetry and microcalorimetry. Both methods showed reasonable agreement, but care was needed to obtain reproducible microcalorimetric results. The PNIPAM samples made by ATRP show a strong tendency to sediment above their LCST, unlike other PNIPAM samples, and hence provide ideal materials for investigating aggregation and colloidal stability phenomena.

As expected, hydrophilic end groups increased the thermal phase transition temperature, while hydrophobic end groups decreased it. This effect is most significant for the shortest chains, where it results in an 8 °C difference in transition temperature upon going from amide to phenylamide end group, at 3 kDa MW. The end group effect diminishes rapidly when MW is above 10 kDa.^{49,50}

The transition temperatures decreased with increasing MW for all four series of samples, as was previously observed with the MCP-initiated PNIPAM. Therefore, in the range of MW and end groups studied, the MW effect dominates over the end group effect. PNIPAM samples bearing an initiator group that is identical to the repeating unit show transition temperatures similar to those bearing methoxypropionate initiator groups reported earlier.³²

The enthalpy of transition was found to decrease slightly with decreasing MW. When approaching the lowest MW, hydrophobic end groups appear to hold the ΔH constant, while the hydrophilic end groups further decrease the ΔH .

Our results show that ATRP can be tuned to give unprecedented control over end group chemistry as well as over molecular weight and molecular weight distribution of PNIPAM, i.e., all three intrinsic factors determining the cloud point of PNIPAM. Properly selected functional initiators or halide end groups may serve as anchor points for peptide and DNA segments, for second polymeric blocks, or for surface attachment. We believe that these approaches will facilitate the use of well-designed PNIPAM blocks in areas ranging from bioconjugates to supported responsive membranes and sensors.

Acknowledgment. We thank Dr. Paul Berti for the use of his UV-vis spectrophotometer and Dr. Richard Epand and Dr. Raquel Epand for the use of their high-sensitivity differential scanning calorimeter. We acknowledge the Natural Sciences and Engineering Research Council of Canada and 3M Canada Inc. for supporting this research.

References and Notes

- (1) Heskins, M.; Guillet, J. E. *J. Macromol. Sci., Chem.* **1968**, A2, 1441–1455.
- (2) Schild, H. G. *Prog. Polym. Sci.* **1992**, 17, 163–249.
- (3) Kubota, K.; Fujishige, S.; Ando, I. *J. Phys. Chem.* **1990**, 94, 5154–5158.
- (4) Wang, X.; Qiu, X.; Wu, C. *Macromolecules* **1998**, 31, 2972–2976.
- (5) Tiktopulo, E. I.; Uversky, V. N.; Lushchik, V. B.; Klenin, S. I.; Bychkova, V. E.; Pitsyn, O. B. *Macromolecules* **1995**, 28, 7519–7524.
- (6) Stayton, P. S.; Shimoboji, T.; Long, C.; Chilkoti, A.; Chen, G.; Harris, J. M.; Hoffman, A. S. *Nature (London)* **1995**, 378, 472–474.
- (7) Umeno, D.; Mori, T.; Maeda, M. *Chem. Commun.* **1998**, 1433–1434.
- (8) Pennadam, S. S.; Lavigne, M. D.; Dutta, C. F.; Firman, K.; Mernagh, D.; Gorecki, D. C.; Alexander, C. *J. Am. Chem. Soc.* **2004**, 126, 13208–13209.
- (9) Hoffman, A. S.; Stayton, P. S. *Macromol. Symp.* **2004**, 207, 139–151.
- (10) Li, C.; Gunari, N.; Fischer, K.; Janshoff, A.; Schmidt, M. *Angew. Chem., Int. Ed.* **2004**, 43, 1101–1104.
- (11) Zhu, M.; Wang, L.; Exarhos, G. J.; Li, A. D. Q. *J. Am. Chem. Soc.* **2004**, 126, 2656–2657.

- (12) Ito, T.; Hioki, T.; Yamaguchi, T.; Shinbo, T.; Nakao, S.; Kimura, S. *J. Am. Chem. Soc.* **2002**, *124*, 7840–7846.
- (13) Sun, T.; Liu, H.; Song, W.; Wang, X.; Jiang, L.; Li, L.; Zhu, D. *Angew. Chem., Int. Ed.* **2004**, *43*, 4663–4666.
- (14) Schild, H. G.; Tirrell, D. A. *J. Phys. Chem.* **1990**, *94*, 4352–4356.
- (15) Aoshima, S.; Oda, H.; Kobayashi, E. *J. Polym. Sci., Part A: Polym. Chem.* **1992**, *30*, 2407–2413.
- (16) Lessard, D. G.; Ousaleh, M.; Zhu, X. X. *Can. J. Chem.* **2001**, *79*, 1870–1874.
- (17) Bütün, V.; Armes, S. P.; Billingham, N. C. *Polymer* **2001**, *42*, 5993–6008.
- (18) Kunugi, S.; Tada, T.; Tanaka, N.; Yamamoto, K.; Akashi, M. *Polym. J.* **2002**, *34*, 383–388.
- (19) Xue, W.; Huglin, M. B.; Jones, T. G. *J. Macromol. Chem. Phys.* **2003**, *204*, 1956–1965.
- (20) Laukkanen, A.; Valtola, L.; Winnik, F. M.; Tenhu, H. *Macromolecules* **2004**, *37*, 2268–2274.
- (21) Tong, Z.; Zeng, F.; Zheng, X. *Macromolecules* **1999**, *32*, 4488–4490.
- (22) Zheng, X.; Tong, Z.; Xie, X.; Zeng, F. *Polym. J.* **1998**, *30*, 284–288.
- (23) Liu, Q.; Yu, Z.; Ni, P. *Colloid Polym. Sci.* **2004**, *282*, 387–393.
- (24) Fujishige, S.; Kubota, K.; Ando, I. *J. Phys. Chem.* **1989**, *93*, 3311–3313.
- (25) Otake, K.; Inomata, H.; Konno, M.; Saito, S. *Macromolecules* **1990**, *23*, 283–289.
- (26) Chung, J. E.; Yokoyama, M.; Aoyagi, T.; Sakurai, Y.; Okano, T. *J. Controlled Release* **1998**, *53*, 119–130.
- (27) Chung, J. E.; Yokoyama, M.; Suzuki, K.; Aoyagi, T.; Sakurai, Y.; Okano, T. *Colloids Surf., B* **1997**, *9*, 37–48.
- (28) Yamazaki, A.; Song, J. M.; Winnik, F. M.; Brash, J. L. *Macromolecules* **1998**, *31*, 109–115.
- (29) Baltes, T.; Garret-Flaudy, F.; Freitag, R. *J. Polym. Sci., Part A: Polym. Chem.* **1999**, *37*, 2977–2989.
- (30) Ringsdorf, H.; Venzmer, J.; Winnik, F. M. *Macromolecules* **1991**, *24*, 1678–1686.
- (31) Kujawa, P.; Winnik, F. M. *Macromolecules* **2001**, *34*, 4130–4135.
- (32) Kujawa, P.; Segui, F.; Shaban, S.; Diab, C.; Okada, Y.; Tanaka, F.; Winnik, F. M. *Macromolecules* **2006**, *39*, 341–348.
- (33) Xia, Y.; Yin, X.; Burke, N. A. D.; Stöver, H. D. H. *Macromolecules* **2005**, *38*, 5937–5943.
- (34) Ciampolini, M.; Nardi, N. *Inorg. Chem.* **1966**, *5*, 41–44.
- (35) Rademacher, J. T.; Baum, M.; Pallack, M. E.; Brittain, W. J.; Simonsick, W. J. *Macromolecules* **2000**, *33*, 284–288.
- (36) Schlesinger, A. H.; Prill, E. J. *J. Am. Chem. Soc.* **1956**, *78*, 6123–6127.
- (37) Sonawane, H. R.; Pol, A. V.; Moghe, P. P.; Sudalai, A.; Biswas, S. S. *Tetrahedron Lett.* **1994**, *35*, 8877–8880.
- (38) Teodorescu, M.; Matyjaszewski, K. *Macromolecules* **1999**, *32*, 4826–4831.
- (39) Teodorescu, M.; Matyjaszewski, K. *Macromol. Rapid Commun.* **2000**, *21*, 190–194.
- (40) Neugebauer, D.; Matyjaszewski, K. *Macromolecules* **2003**, *36*, 2598–2603.
- (41) Yin, X.; Stöver, H. D. H. *Macromolecules* **2005**, *38*, 2109–2115.
- (42) Schilli, C.; Lanzendörfer, M. G.; Müller, A. H. E. *Macromolecules* **2002**, *35*, 6819–6827.
- (43) Tiktopulo, E. I.; Bychkova, V. E.; Rička, J.; Ptitsyn, O. B. *Macromolecules* **1994**, *27*, 2879–2882.
- (44) Diab, C.; Akiyama, Y.; Kataoka, K.; Winnik, F. M. *Macromolecules* **2004**, *37*, 2556–2562.
- (45) Mikheeva, L. M.; Grinberg, N. V.; Mashkevich, A. Y.; Grinberg, V. Y.; Thanh, L. T. M.; Makhaeva, E. E.; Khokhlov, A. R. *Macromolecules* **1997**, *30*, 2693–2699.
- (46) Ding, Y.; Ye, X.; Zhang, G. *Macromolecules* **2005**, *38*, 904–908.
- (47) Chan, K.; Pelton, R.; Zhang, J. *Langmuir* **1999**, *15*, 4018–4020.
- (48) Gorelov, A. V.; Du Chesne, A.; Dawson, K. A. *Physica A* **1997**, *240*, 443–452.
- (49) Li, M.; Wu, C. *Macromolecules* **1999**, *32*, 4311–4316.
- (50) A paper describing the thermal properties of pyrenyl end-functionalized PNIPAM prepared by ATRP appeared after this manuscript was accepted. Duan, Q.; Miura, Y.; Narumi, A.; Shen, X.; Sato, S.-I.; Satoh, T.; Kakuchi, T. *J. Polym. Sci., Part A: Polym. Chem.* **2006**, *44*, 1117–1124. The cloud point of the narrow-disperse PNIPAM samples increased by almost 8 °C as M_n increased from 3000 to 5000 Da, likely because of the large hydrophobic pyrenyl end group.
- (51) A paper describing the thermal properties of several end-functionalized PNIPAM samples obtained by azo-initiated polymerization followed by mass fractionation appeared after this manuscript was accepted. Furyk, S.; Zhang, Y.; Ortiz-Acosta, D.; Cremer, P. S.; Bergbreiter, D. E. *J. Polym. Sci., Part A: Polym. Chem.* **2006**, *44*, 1492–1501. The cloud points of the PNIPAM samples were insensitive to MW when M_w was above ~100 kDa. At lower MW (M_w ~20–100 kDa), there was a small decrease for samples with a hydrophobic trityl end group and a small increase for those with an isobutyronitrile end group. This is consistent with both MW and end-group effects being most important for low MW samples (<20 kDa).

MA0519617